STATISTICAL DESCRIPTION OF TURBULENT AXISYMMETRIC IMPINGING JET WITH EXCITED COHERENT STRUCTURES

Sergey Alekseenko, Artur Bilsky, Oksana Heinz,

Boris Ilyushin, Dmitriy Markovich, Victor Vasechkin

Institute of Thermophysics Siberian Branch of RAS

Lavrentyev Ave., 1, Novosibirsk, 630090, Russia

dmark@itp.nsc.ru

ABSTRACT

The statistical characteristics of axisymmetric submerged impinging jet are experimentally determined for conditions of external periodical forcing. The method of conditional sampling is used together with electrodiffusion technique and PIV. The triple decomposition of velocity and skin friction pulsations is applied in order to distinguish the coherent and random parts of turbulent kinetic energy and statistical characteristics. The major contribution of coherent component is ascertained.

INTRODUCTION

Impinging jets are the hydrodynamical objects which are often used for the validation of elaborating CFD. This is because such flows are wide spread in the technology (jet heating, cooling, drying, aircraft engines) and nature (microbursts etc.). Besides, the impinging jets are the objects with wide spectrum of physical effects, providing this kind of flow by universal test for modelling. In different flow regions one can observe both free and wall shear layers, large-scale vortex structures (LSVS) developing in the free jet and interacting with the impingement surface, sharp curvature of stream lines in the vicinity of jet turn and, as a consequence, appearance of Gortler instability. PDF of turbulent fluctuations in impinging jet is far from the Gauss distribution due to the presence of LSVS and anisotropy of pulsations in the near-wall region is quite different from one at usual boundary layer conditions.

There are only few experimental studies of impinging jet hydrodynamics, which are traditionally used for testing of mathematical models. Thus, enough complete information on the main turbulent characteristics is presented in the paper by Cooper et al. (1993) where authors performed hot-wire measurements of average velocity components, RMS pulsations and Reynolds stresses for the jet issuing from round tube and impinging on the normal obstacle. Landreth and Adrian (1990) presented data on the PIV measurements of impinging jet characteristics. Their results contained instant distributions of velocity and vorticity in the central cross-section of the jet and also ensemble averaged velocity field in the neighbourhood of stagnation point. Triple correlations were measured with the aid of PTV in the work of Nishino et al. (1996). In all these studies impinging jet was considered in its natural conditions. Practically only work by Didden and Ho (1985) contains the results on conditionally averaged velocity components in boundary layer of radial wall region of forced impinging jet. Local unsteady separations of boundary layer were registered which were induced by large vortices penetrating into wall region. However, the presented information was restricted by mean characteristics.

In order to create the complete pattern of the large-scale coherent structures development in the impinging jet shear layer the information is needed about the "frozen structure" of these vortex formations. For this aim the conditions should be realised when the large-scale structures are excited by external forcing and conditional sampling technique needs to be used for data processing. At the same time for the validation of mathematical models the comparison on statistical moments of different order is necessary to describe adequately the mixing and transfer processes. Along with this reasons an accurate experimental information will allow more understanding of the physical mechanisms of instabilities development and energy transfer between different turbulent scales.

This work is devoted to the experimental study of

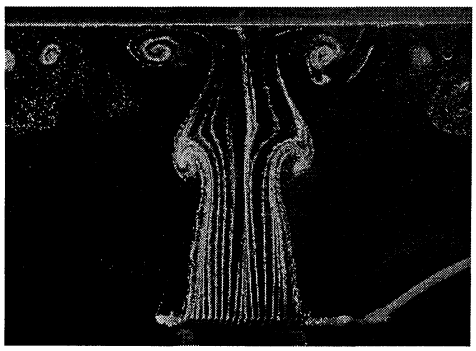

Figure 1 : The photograph of impinging jet flow. Re = 1400, H/d = 3, Sh = 0.5.

submerged axisymmetric impinging jet hydrodynamics under the conditions of external periodical forcing with the frequencies from the range of most sensitivity of a jet shear layer.

DESCRIPTION OF EXPERIMENT

The experiments were carried out at the hydrodynamical loop with exchangeable working sections (plexiglas channels) for using different experimental techniques. The set up was equipped by the system of pumps and flow meters, reservoir, connecting tubes and apparatus for measurements. Well-profiled round nozzles with diameters of 10 and 15 mm were inserted through the side (or bottom) wall of a channel. The submerged round jet issuing from the nozzle impinged normally on the opposite wall.

To measure wall shear stress and local liquid velocities the electrodiffusion method (EDM) was applied. The details of this technique are described in the author's work (Alekseenko and Markovich, 1994). The skin friction probes were placed at the measuring plate (moving wall of the channel) which could be shifted and this allowed to change the radial position of each probe with an accuracy of 0.1 mm. Velocity probes were inserted through the wall side. The electrical signals from the probes passed to the a.d. transformer through the d.c. amplifiers. A complete data processing was accomplished by a PC.

Measurements of instant velocity fields were performed using 2D PIV system (Dantec FlowMap PIV System based on PIV1100 processor, ES 1.0 Kodak camera 1K x 1K and 50 mJ NdYAG laser). The software developed allows to calculate the statistical characteristics of turbulent flow of impinging jet including high-order statistical moments. To obtain more precise estimation of high statistical moments the large number of instant frames of velocity distributions were processed (up to 9,000 for separate phase and 20,000 for whole statistics). The spatial resolution in present experiments was 1.1 mm.

The excitation of the jet was provided by a standard electrodynamic vibration exciter connected by the instrumentality of the silphone with the plenum chamber. The sinusoidal excitant signals conveyed from the generator through the power amplifier to the exciter. The initial oscillations of flow embodied the axisymmetric mode (m = 0) and their RMS value changed from $\tilde{u}/U_0 = \sqrt{\tilde{u}^2}/U_0$ = 0.0001 to 0.03 depending on the experimental conditions. The forcing frequency f_f, was characterized by the Strouhal number, $\mathrm{Sh_d} = f_f \cdot d/U_0$.

The velocity measurements near the nozzle exit, performed for high values of Reynolds number, have shown that the imposed oscillations of lowest level do not influence the initial flow characteristics. The level of natural turbulence measured in the vicinity of nozzle exit was for different nozzles in the range

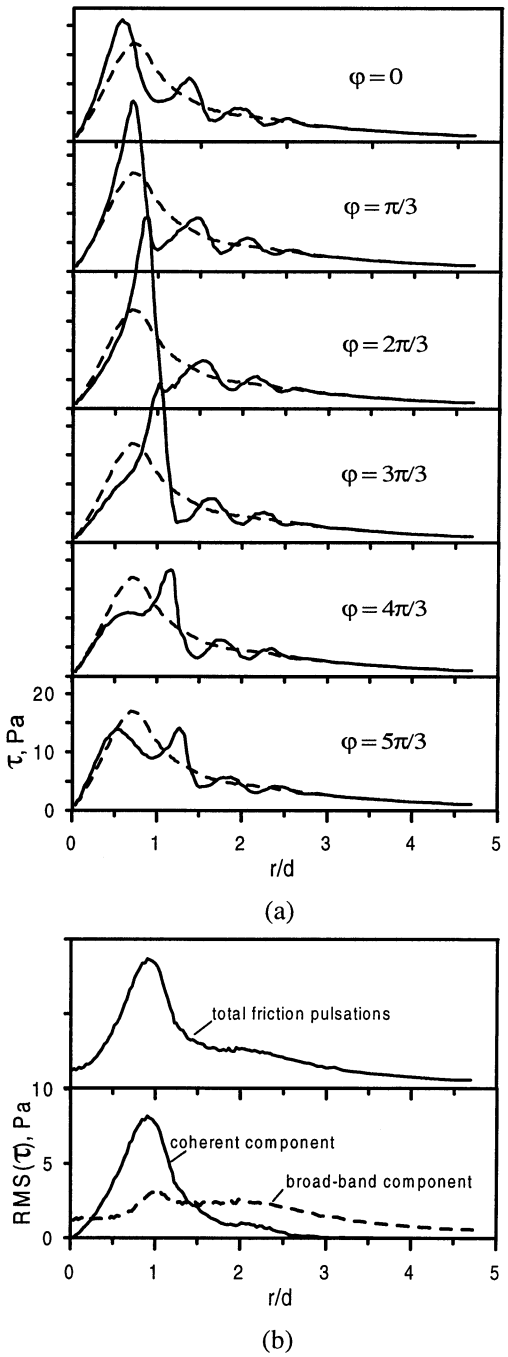

Figure 2 : Conditionally averaged distributions of wall shear stress (a) and decomposition of its RMS pulsations onto coherent and broad-band components. EDM measurements. Re = 12700, H/d = 2, d = 10 mm, Sh = 0.53.

of $u'/U_0 = \sqrt{\overline{u'^2}}/U_0$ = 0.005 ÷ 0.06 at the nozzle axis and 0.05 ÷ 0.1 at the centre of shear layer.

During the experiments the range of Reynolds numbers was tested: Re = 7600 ÷ 25200. Here $\mathrm{Re} = U_0 \cdot d/\nu$, U_0 is the mean flow rate velocity at the nozzle exit, d is the nozzle diameter and ν is the kinematic viscosity of electrochemical solution equal

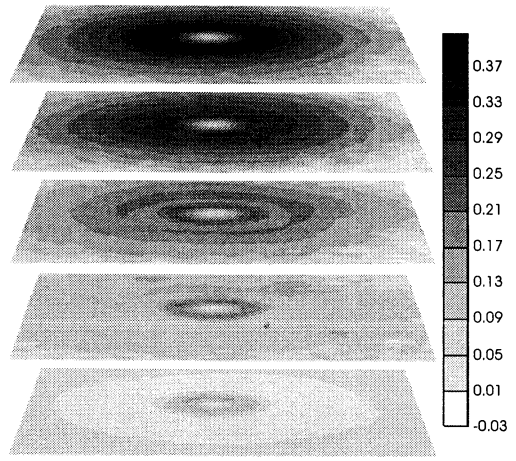

(a)

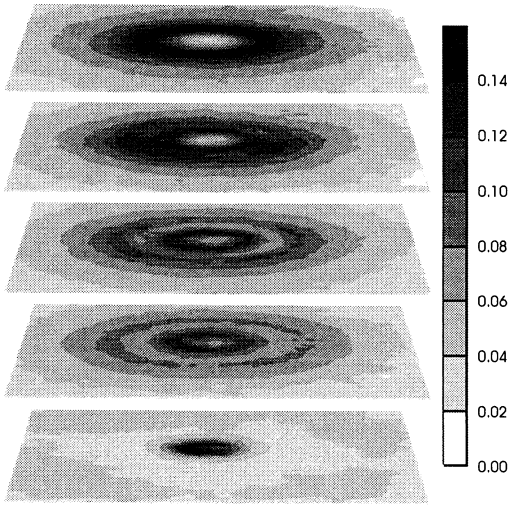

(b)

Figure 3 : Distributions of radial velocity component in near-wall horizontal cross-sections. Re = 7600, H/d = 3, d = 15 mm, Sh = 0.5. Upper cross-section: z = 1 mm, lower - 5 mm. (a) - mean radial velocity V_r , (m/s), (b) - RMS pulsations of radial velocity $\sqrt{\overline{V_r'^2}}$, (m/s).

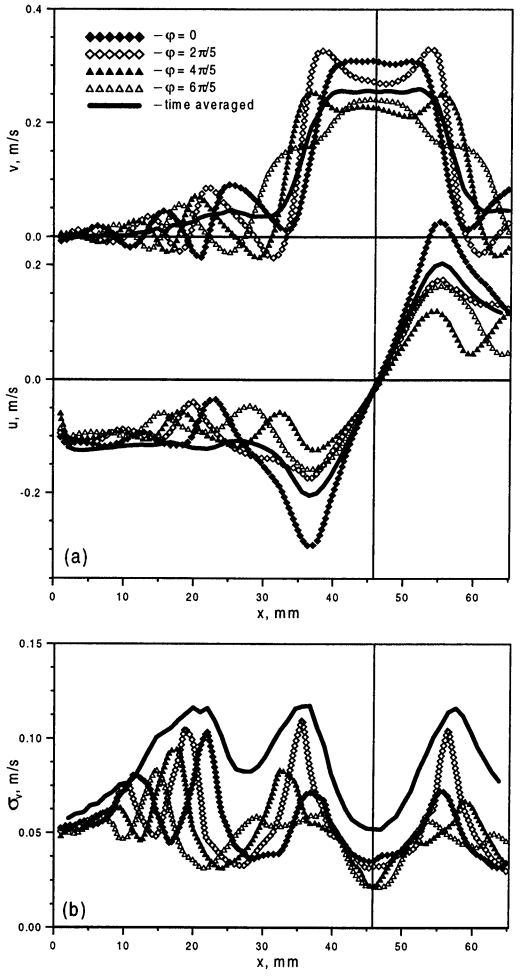

Figure 4 : Phase averaged distributions of velocity components (a) and dispersion σ_v (b) in horisontal cross-section of the flow: z = 3.1 mm. PIV measurements. Flow conditions as in Fig. 3.

to $1.04 \cdot 10^{-6}$ m^2/s. The non-dimension distance H/d between the edge of a nozzle and the plate was varied from 2 to 4.

RESULTS AND DISCUSSION

The impinging jet flow under the conditions of periodic forcing with the frequencies from the range of most jet's sensitivity (Sh = 0.4 ÷ 0.7) is strictly periodic in the near field of the jet with well pronounced large scale vortex structures (Alekseenko et al., 1997). This fact allowed us to perform the triple decomposition of velocity and wall shear stress pulsations in order to separate the coherent and broadband components of physical quantities. According the common approach (Evans, 1975, Yule, 1977) the triple decomposition for instant value of generalised variable a is (Hussain and Reynolds, 1972):

$$a(\vec{x},t) = \overline{a}(\vec{x}) + \tilde{a}(\vec{x},t) + a'(\vec{x},t),$$

where first, second and third terms in the left part of equation are correspondingly time average, coherent (periodic) and stochastic components of pulsations. In the present work the velocity and wall shear stress components were considered as partial cases of a. Phase averaging gives the following:

$$\langle a(\vec{x},t_i)\rangle = a(\vec{x}) + \tilde{a}(\vec{x},t_i) = \lim_{N\to\infty}\frac{1}{N}\sum_{k=1}^{N} a_k(t_i)$$

It is equivalent to the average value a for each phase of the flow. In EDM experiments the probe signal was divided into cycles according excitation frequency. For N pulsation cycles, the ensemble average at time instant t_i from the beginning of a cycle was calculated for velocity and friction components

and their squares. $a_k(t_i)$ is the physical value reading in the k^{th} cycle at time t_i. For PIV measurements the conditional sampling was provided by synchronisation of excitant signal with laser pulses and setting corresponding phase delay. Both centered and non-centered (relative to time average values) characteristics were calculated.

The set of statistical characteristics including 2nd, 3rd and 4th order moments has been calculated for a number of flow phases: 100 phases for EDM wall shear stress and velocity measurements and 20 phases for whole velocity field (PIV experiments) were tested. The number of samples, processed for each phase was varied from 1000 to 9000 in different experiments. Figure 2, a shows the phase averaged distributions of wall shear stress along impingement surface (solid lines). Dashed lines correspond to the whole averaged value. Six equidistant phases from 100 are plotted. It is clearly seen from the figure that local values of skin friction can be extremely large owing to coherent structures influence. In Fig. 2, b the decomposition of pulsations level on coherent and stochastic parts is presented. In the vicinity of stagnation point the coherent component of skin friction pulsations dominates whereas in the far field of the radial wall jet the broad-band component yields a major contribution into whole turbulence level.

The analysis of flow structure was performed also on the basis of measurements of local flow velocities in the horizontal near-wall cross sections. These results are presented in Fig. 3, a for time averaged radial velocity component and in Fig. 3, b for its RMS deviation. In the horizontal cross-sections the polar coordinates are used for data processing. The typical nonmonotonical shape of velocity profiles can be observed in different cross-sections of flow. Along radial coordinate the velocity initially grows from zero at critical point up to maximum at some radial distance and then decreases with further increase of r. However at some intermediate range of axial coordinate z (point of origin - impingement plane) one can observe the appearance of second local maximum of velocity and, correspondingly, maximum of pulsations level (Figure 3, b, third cross section, $z = 3$ mm) which is more pronounced. Such nonmonotonical behaviour of these distributions can be explained on the basis of analysis of nonlinear contribution of large-scale structures, propagating along the wall, into flow characteristics. The tangential component of velocity is negligible both for instant and whole averaged distributions and so these data are not presented in the paper. The example of conditionally averaged values of velocity components and fluctuation level for different flow phases is shown in Fig. 4, a, b for near-wall horizontal cross section. This Figure presents the distributions of "frozen" velocity components. The periodical spatial structure of phase-locked flow is demonstrated.

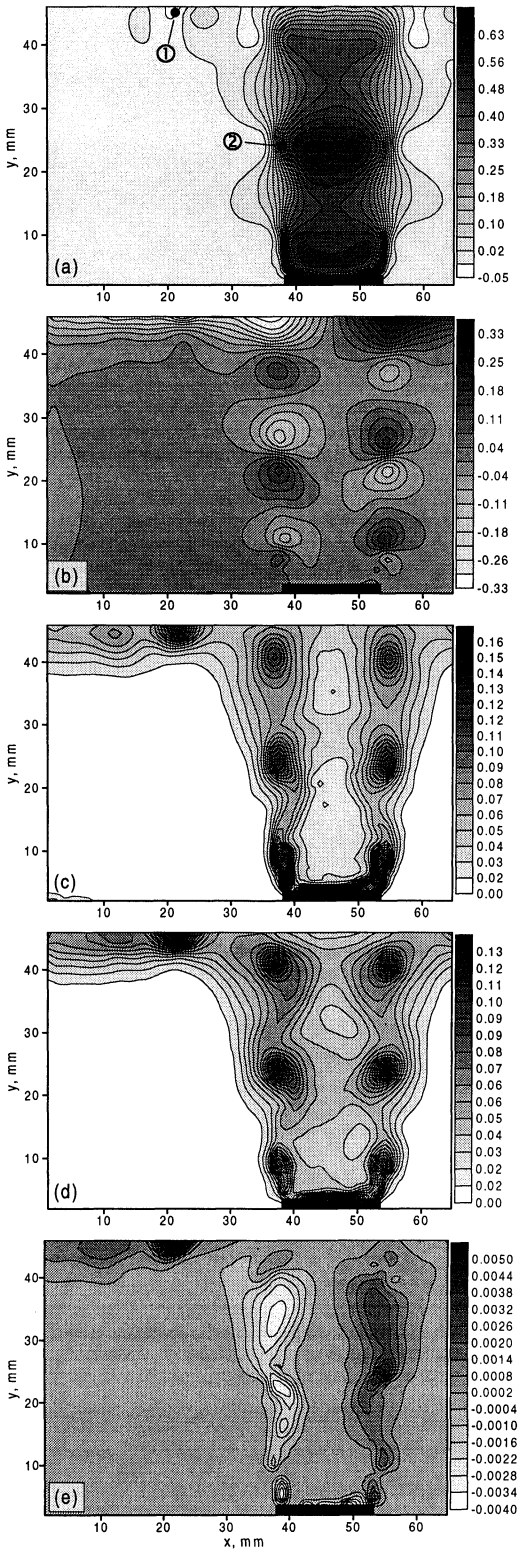

Figure 5 : Spatial distributions of conditionally averaged characteristics of impinging jet flow field. PIV measurements. Flow conditions as in Fig. 3. (a), (b) - v and u velocity components, (c), (d) - components of velocity dispersion - σ_v, σ_u, (e) - Reynolds stresses. Averaging over 9000 instant frames of velocity field recording at the same phase. Level of flow excitation is $\tilde{u}/U_0 = 0.03$.

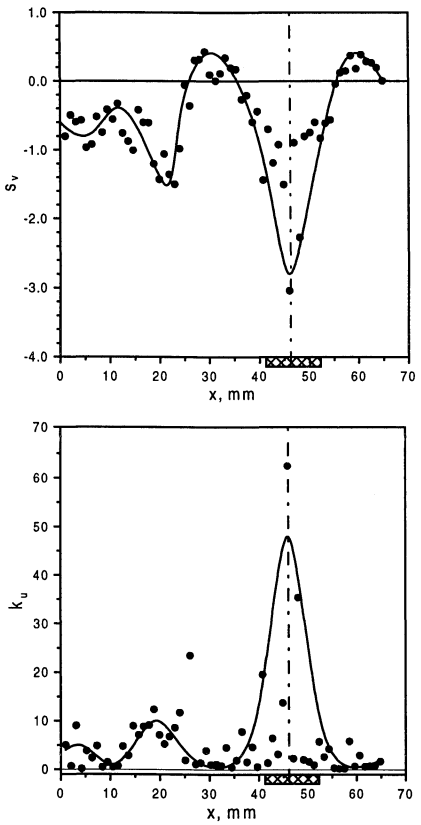

Figure 6 : Phase averaged distributions of high order moments in horizontal cross-section of the flow. $z = 3.1$ mm. PIV measurements. Flow conditions as in Fig. 3. The same phase as in Fig. 5.

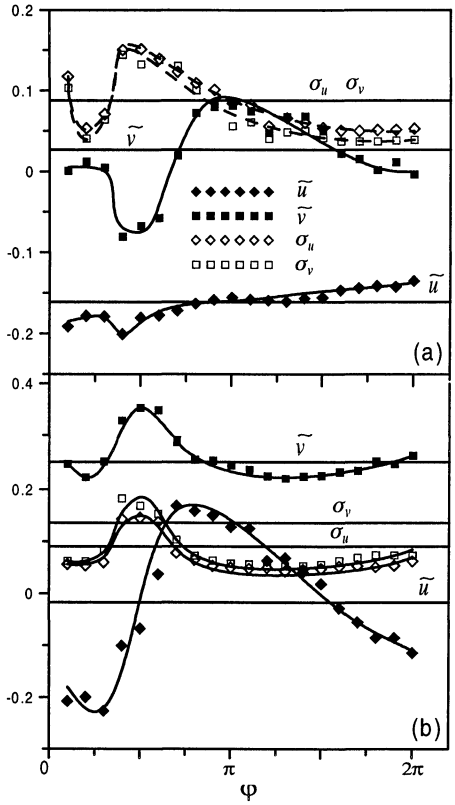

Figure 7 : Velocity and dispersion components changing during one period of structure propagation. Experimental conditions as above. (a) - point 1 - $x_0/d = 1.7$, $z = 2$ mm, (b) - point 2 - $x_0/d = 0.57$, $z = 23.4$ mm.

Similar to Fig. 3, b the double-maximum of whole averaged distributions for pulsations level can be observed.

Figure 5 presents the phase averaged distributions of velocity components, their dispersion and Reynolds stress. The averaging for selected phase was performed with using 9000 fields of velocity vectors. Presented distributions show the "frozen structure" of the flow, averaged only over the stochastic part of turbulent pulsations. One can clearly observe the periodic spatial flow structure caused by large vortices. The areas with maximum values of second moment of velocity pulsations (Fig. 5, c, d) correspond to the regions with large velocity gradients (Fig. 5, a, b). The distribution of Reynolds stress is also strong nonuniform with locations of maximums in the centre of mixing layer.

The observed early phenomenon (Didden and Ho, 1985, Alekseenko and Markovich, 1994) - appearance of small secondary vortex in the near-wall region was directly registered by PIV velocity measurements (see Fig. 5, a - vicinity of zone 1). It is characterised by negative velocity values and is caused by local pressure gradient induced by propagating large vortex. This vortex is clearly seen in the phase averaged second order moments distributions (Fig. 5, c-e).

The high order moments of velocity pulsations were calculated for different flow phases as well as for whole ensemble of instant velocity fields. The examples of asymmetry and excess coefficients calculated for chosen phase of flow are shown in Fig. 6. These distributions for near-wall horizontal cross-section also reflect the periodical structure of the flow and most distinction from zero values, corresponding to Gauss PDF, is observed in the vicinity of large vortices location for considered phase. The large scatter in the high moments data is caused by PIV technique errors and so more sophisticated filtration and validation methods should be developed and integrated into commercial DANTEC software.

Figure 7 presents the phase averaged time evolution of velocity components and their dispersions during one period of structure's propagation. The results for two most distinctive points of flow are presented (points 1 and 2 in Fig. 5, a). The straight lines represent the whole averaged values. It should be noted that flow characteristics change not evenly during structure's period and certain range of phases exists (from $\pi/8$ to $3\pi/4$ for given conditions) with most strong variation of physical values. This fact represents the manifestation of nonlinear character of large-scale structures in the flow.

The information about phase evolution is given also in Fig. 8. The measured PDFs of two velocity

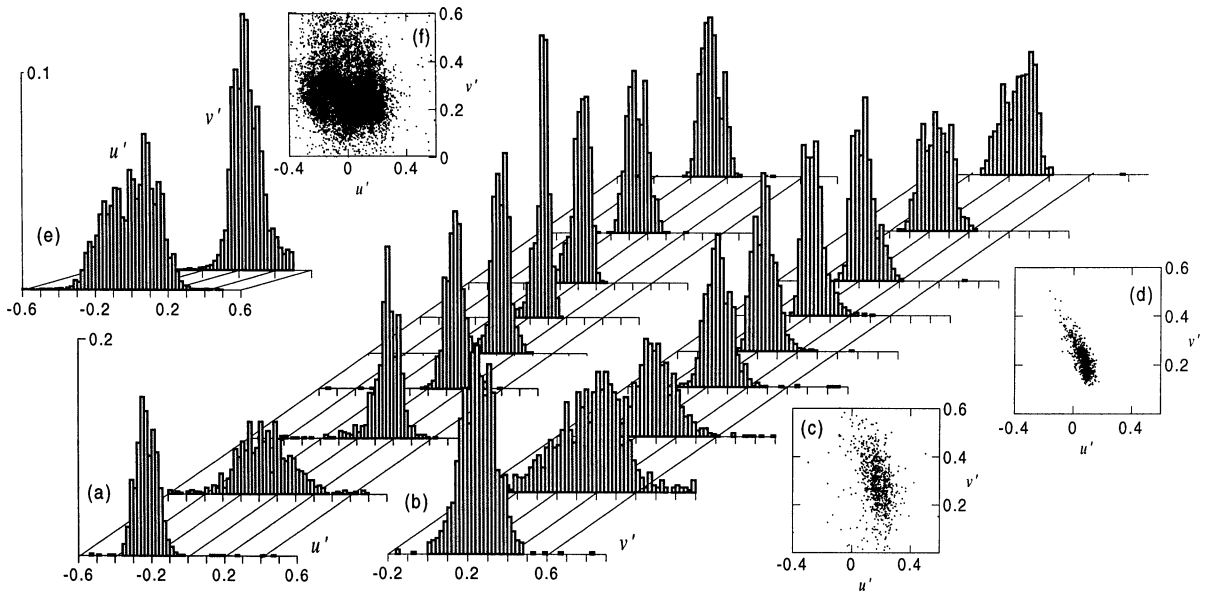

Figure 8 : Histograms of velocity pulsations and phase planes. Measuring point N2 - x_0 = 8.55 mm (x_0/d = 0.57), z = 23.4 mm (z/d = 1.56). Re = 7600, H/d = 3, d = 15 mm, Sh = 0.5. (a), (b) - conditionally sampled histograms, (c), (d) - conditionally sampled phase planes for 3rd and 6th phases (from below), (e), (f) - whole statistics (20,000 instant frames).

components (Fig. 8, a, b) are presented for structure's propagation period separated into nine equidistant phases. Example is adduced for the centre of shear layer in developing free jet (point 2 in Fig. 5, a). The simultaneous plotting of histograms for two velocity components at the same phase allows to observe the local anisotropy of pulsations (see also conditionally sampled phase planes). At the same time for whole statistics (Fig.8, e, f) the anisotropy of pulsations is not pronounced.

CONCLUSION

The statistical analysis was performed for the characteristics of axisymmetrical submerged impinging jet at natural conditions and under the action of external forcing at the frequencies from the range of most jet's sensitivity. On the basis of electrodiffusion and PIV measurements and conditional sampling technique the phase averaged flow characteristics were determined. The major contribution of coherent component into main flow characteristics was shown. The strong anisotropy of phase-locked pulsations was observed while whole statistical quantities can have substantially more isotropic character.

ACKNOWLEDGMENTS

This work was supported by INTAS grant 97-2022 and RFBR grants 00-01-00821, 00-15-96810 and 01-02-17662.

REFERENCES

Alekseenko, S.V. and Markovich, D.M., 1994. "Electrodiffusion diagnostic of wall shear stresses in impinging jets", J. Appl. Electrochemistry, vol. 24, pp. 626-631.

Alekseenko, S.V., Markovich, D.M. and Semenov, V.I., 1997, "Effect of external disturbances on the impinging jet structure", Proc. of the 4th World Conference on Experimental Heat Transfer, Fluid Mech. and Thermodynamics, Brussels, June 2-6, vol. 3, pp. 1815-1822.

Cooper, D., Jackson, D. C., Launder, B. E. and Liao, G. X., 1993, "Impinging jet studies for turbulence model assessment - I. Flow-field experiments", Int. J. Heat Mass Transfer, vol. 36, pp. 2675-2684.

Didden, N. and Ho, C.-M., 1985, "Unsteady separation in a boundary layer produced by an impinging jet", J. Fluid Mech., vol. 160, pp. 235-256.

Evans, R. L., 1975, "Turbulence and unsteadiness measurements downstream of a moving blade row", ASME Journal of Engineering and Power, vol. 97, pp. 131-139.

Hussain, A. K. F. M., and Reynolds, W. C., 1972, "The mechanics of an organized wave in turbulent shear flow. Part 2, experimental results", J. of Fluid Mech., vol. 54, pp. 241-261.

Landreth, C.C. and Adrian, R.J., 1990, "Impingement of a low Reynolds number turbulent circular jet onto a flat plate at normal incidence", Experiments in Fluids, vol. 9, pp. 74-84.

Nishino, K., Samada, M., Kasuya, K. and Torii, K., 1996. "Turbulence statistics in the stagnation region of an axisymmetric impinging jet flow", Int. J. Heat and Fluid Flow, vol. 17, pp. 193-201.

Yule, A. J., 1978, "Large-scale structure in the mixing layer of a round jet", J. of Fluid Mech., vol. 89, pp. 413-432.